galaxies

MDPI

Article

Multiplicity of Luminous Blue Variable Stars

A. Lobel * and N. Gorlova

Royal Observatory of Belgium, Ringlaan 2, B-1180 Brussels, Belgium
* Correspondence: alobel@sdf.org or alex.lobel@oma.be

Abstract: The study of Luminous Blue Variables (LBVs) is critical to understanding the mechanisms behind their recurring S Dor-like outbursts, which can span decades and feature dramatic spectral changes. These outbursts may result from atmospheric instability or interactions with a companion star, but their causes remain poorly understood. Detecting binarity in LBVs through long-term radial velocity (RV) measurements, which can identify orbital motion via shifts in absorption lines, is a promising method. Periodic line shifts and variability can reveal the presence of a companion star. We report on the monitoring of four LBVs and two candidate LBVs (cLBVs), observing high-resolution spectra from 2009 to 2024. Although we do not find a clear periodic RV signal for LBVs MWC 930, P Cyg, or HD 168607, our long-term monitoring campaign previously detected the binarity of cLBV MWC 314 in 2013. For the first time, we detected a periodic signal in the RV data of the cLBV Schulte 12. In addition, in LBV HD 168607, we observed Discrete Absorption Components, indicative of large-scale structures in a rotating wind. These findings advance our understanding of the binary nature of LBVs and their complex outburst behaviors.

Keywords: massive stars; binaries; stellar winds; outbursts; spectroscopy; radial velocity; monitoring

check for updates

Academic Editors: Sergei Zharikov, Serik Khokhlov and Anatoly Miroshnichenko

Received: 28 February 2025
Revised: 24 March 2025
Accepted: 25 March 2025
Published: 28 March 2025

Citation: Lobel, A.; Gorlova, N. Multiplicity of Luminous Blue Variable Stars. *Galaxies* **2025**, *13*, 29. https://doi.org/10.3390/galaxies13020029

Copyright: © 2025 by the authors. Licensee MDPI, Basel, Switzerland. This article is an open access article distributed under the terms and conditions of the Creative Commons Attribution (CC BY) license (https://creativecommons.org/licenses/by/4.0/).

1. Introduction

Luminous Blue Variables (LBVs) are among the most fascinating and enigmatic stars in the universe. They represent an extreme phase in the life of massive hot stars known for their high luminosity and dramatic variability. LBVs are best characterized by recurring outbursts, which result in large and rapid variations in visual brightness (V) and surface temperature ($T_{\rm eff}$). These outburst events challenge our understanding of stellar evolution, as they appear to be tied to a physical instability mechanism operating in very massive stars, which is not yet fully understood. The exact cause of LBV outbursts is subject to active research. Current theory suggests both intrinsic stellar (atmospheric) instability and external factors, such as possible interactions with companion stars. Understanding LBVs is crucial because their unusual properties provide insights into the late stages of stellar evolution, in particular of the most massive stars that play a key role in enriching galaxies with heavy elements through supernova (SN) explosions. The general review by [1] outlined the idea that LBVs could be undergoing internal pulsations or thermal instabilities, possibly driven by changes in the core structure. It also suggested that strong LBV variability could result from a combination of intrinsic stellar processes and possible interactions with companion stars. Ref. [2] discusses how LBVs are at a crucial transition between different evolutionary phases, such as from blue OB-type supergiants to Wolf-Rayet (W-R) stars, with (eruptive) variability likely arising from pulsational instability or due to binary interactions, for example due to mass transfer under Roche overflow.

LBVs are characterized by high mass loss rates and powerful stellar winds with outflow velocities ranging from 200 km s^{-1} to over 2000 km s^{-1}. The mass loss rates are typically a few 10^{-5} to 10^{-3} $M_{\odot}y^{-1}$. They eject material during major outburst events that can form large circumstellar nebulae, such as the Homunculus Nebula of η Car during its Great Eruption in the 1840s. LBVs are thought to represent a brief and unstable phase in the evolution of the most massive hot stars (of ∼50 to 100 Ky), while transitioning between a more stable phase as OB-type supergiants and their eventual evolution into W-R stars or into core-collapse SNe. As such, LBVs may be progenitors of type IIn SNe, a subclass of SNs with narrow emission lines typically associated with the interaction of the SN explosion with the surrounding stellar wind. A good number of LBVs are also identified in the LMC, SMC, and M31, often inside star-forming regions, important for the role these massive hot stars play in metal-poor environments [3].

LBVs reveal unpredictable photometric, polarimetric, and spectroscopic variability on timescales of decades, which we indicate with "S Dor-type" variability addressed in this paper. S Dor-type variability is recurrent and characterized by irregular V-band changes with typical amplitudes of 1 to 2 magnitudes that correspond to changes of up to ∼15,000 K in $T_{\rm eff}$, and to a factor of ten in the hydrostatic stellar radius [4]. During visual minima, LBVs are typically hotter, while for visual maxima, lower $T_{\rm eff}$ values are observed (e.g., [5]). These brightness cycles are observed in the S Dor variables, P Cygni, Hubble-Sandage variables, and other similar stars generally called LBVs [6]. The physical mechanisms responsible for this S Dor-type variability are presently not understood, although binarity/multiplicity [7] and global atmospheric dynamic instability [8] have been proposed to play an important role. Note that these S Dor-type cycles should be distinguished from the so-called "giant LBV eruptions", mostly used to indicate the large historical outbursts of η Car and of P Cyg of over 5 magnitudes in V in the 17th century.

In binary systems, gravitational interactions can lead to the vigorous transfer of mass. For example, the stellar wind outflow from the more massive LBV primary could be accreted by a companion star. As a result, the less massive companion can overflow its Roche surface, leading to unstable mass transfer and potentially triggering episodic S Dor-type outbursts [9]. The more compact companion can accrete part of the copious wind mass from the primary, which also enhances the mass loss and causes recurring eruptions. In close or eccentric binary systems, temporal tidal interactions can perturb the primary's outer layers, producing atmospheric instabilities that initiate dramatic variability in both V and $T_{\rm eff}$ [10]. A significant fraction of the 20 bona fide LBVs and ∼40 candidate LBVs (cLBVs) currently known in the galaxy are, in fact, found in binary or multiple star systems. About 60% to 70% are observed in binary systems [11]. However, comparably large binary percentages are also found in O-type stars (>70%; [12]) thought to precede the LBV stage, while binarity is also detected in over 50% of the B-stars [13,14]. Note also that ∼70% of the W-R (WC) stars are found in binaries [15]. The binary fraction containing red supergiants (RSgs) is, however, considerably smaller, being ∼15% [16].

It is important to point out that for a considerable number of bona fide LBVs (showing past outbursts), there are currently no publications supporting binarity. For example, S Doradus, P Cygni, HD 168607, and MWC 930 have been studied for decades without showing credible evidence of binarity/multiplicity. It indicates that not all LBV outbursts (e.g., S Dor-type variability) can be solely attributed to binary interactions [17,18]. One of the most powerful ways of investigating LBV properties is the combination of photometric and spectroscopic monitoring over extended periods of time. Photometric observations reveal long-term brightness variations, while co-eval spectra provide detailed information about the thermal and dynamic processes in the stellar wind and atmosphere.

High-resolution spectroscopy, in particular, is used for radial velocity (RV) measurements of selected spectral lines, offering crucial information about periodic LBV movements and, hence, can reveal the presence/absence of companion stars that would remain unobserved with direct or interferometric imaging techniques. The high-resolution spectroscopic monitoring of LBVs is, however, challenging and requires dedicated long-term observation campaigns, often spanning decades. S Dor-type outbursts are typically irregular and can occur on timescales of a few years to decades. Obtaining complete datasets for tracking the RV variations in c/LBVs requires sustained observation campaigns and advanced analysis methods. The detailed analysis of high-resolution spectra is paramount for detecting the subtle RV variations that can be indicative of orbital motion. If *periodic* RV variations are observed, this provides strong evidence that the LBV is in a (*spectroscopic*) binary system.

In this paper, we present a spectroscopic study of four bona fide LBVs (S Doradus, P Cygni, MWC 930, HD 168607) and one cLBV (Schulte 12). We discuss these stars in the context of a larger ongoing investigation of 10 LBVs and 5 cLBVs. These c/LBVs have been studied in recent years with a variety of methods that involve spectroscopy, photometry, interferometry, adaptive optics (AO) imaging, and X-ray fluxes and spectra. We present the results of a long-term, sustained high-resolution spectroscopic monitoring campaign in the last 15 years using Mercator-HERMES [19]. In Section 2, we summarize the spectroscopic datasets. Section 3 discusses our spectroscopic analysis methods. In Section 4, we present a discussion and the conclusions.

2. Observations

Table 1 summarizes high-resolution observations of 4 LBVs and 3 cLBVs. Each of them has been observed with Mercator-HERMES since 2009 with a large spectral resolution (R = 80,000), except for S Dor, which is in the LMC. The HERMES LBV monitoring spectra are combined with the spectra of other high-resolution spectrographs that we retrieved from a wide variety of online telescope archives. The last column in the table lists the number of spectra obtained for one night of observation time. In most cases, these nightly spectra result from subsequent exposures (of typically 1800 s) that are co-added for improving the spectral signal-to-noise ratio (SNR) in different wavelength regions depending on the star's brightness and spectral type, and most importantly, the selected (sets of) spectral line(s) of interest for our measurements and analysis method.

Table 1. List of the 4 LBVs and 3 cLBVs with high-resolution spectra we combined with continuous long-term monitoring using Mercator-HERMES (since 2009). Note that S Dor in the LMC has no HERMES spectra.

Name	HD	V	Spectral Type	No. of HERMES Nights
S Dor (LMC)	35343	10.2	LBV B3	(5)
MWC 930	-	11.0	LBV B6	22
P Cyg	193237	4.8	LBV B2	36
V4029 Sgr	168607	8.2	LBV B9	27
V4030 Sgr	168625	8.4	cLBV B6	30
MWC 314	-	9.9	cLBV B3	21
Schulte 12	-	11.1	cLBV B2	28

Figure 1 shows the galactic target stars of Table 1 in the upper H-R diagram (blue symbols). The dotted lines drawn between the symbols mark large $T_{\rm eff}$-variations caused by dramatic spectral changes due to S Dor-type variability observed in LBVs AG Car, Westerlund-1 243, HR Car, MWC 930, and HD 160529. Other stars such as HD 168625, Schulte 12, MWC 314, and Pistol have not shown this type of large variability so far but reveal high-resolution B-star spectra very similar to the bona fide LBVs. These stars,

therefore, are sometimes called "dormant LBVs". They are possibly bona fide LBVs in a quiescent state, which we indicate with cLBV. The 5 galactic c/LBVs in Figure 1 and Table 1 monitored with HERMES are as follows: MWC 314, P Cyg, MWC 930, HD 168625, and HD 168607, and they are marked with large squared symbols. We also monitored Schulte 12; however, the high luminosity for the reddening and distance to this cLBV is currently debated in the literature. Ref. [20], in their Figure 12, place Schulte 12 above the HD limit for a very luminous star. However, Ref. [21] more recently argued that Schulte 12 is a much less luminous cLBV below the HD limit based on the Gaia EDR3 parallax. The LBVs are frequently observed in circumstellar bi-polar, spherical, and non-spherical nebulae, signaling major mass ejection events in the past. This is also the case for most cLBVs (see also Table 2), except for Schulte 12 in the Cyg OB2 association, where no nebula is imaged towards this remarkable highly reddened star.

Table 2. A sample of the 10 LBVs and 5 cLBVs we investigated in part based on long-term high-resolution spectroscopic observations with Mercator-HERMES (since 2009). The bold face letters indicate the results of our search for periodicity in RV time series of the selected spectral lines we discuss for the LBVs S Dor, MWC 930, P Cygni, and HD 168607 and the cLBV Schulte 12.

Name	Spectral Type	Orbital Elements	Spectroscopic Binary	Imaging Binary	Nebula Morphology	X-Rays
10 LBVs						
Eta Car	B + O/WR	Y [1]	Y [2]	Y [3]	large bipolar	Y
HR Car	B + RSg?	Y [4]	Y [5]	Y [4]	bipolar	
Wd-1 243	B/A3	N	N	N		Y
AG Car	B2/3	N	N	N	non-spherical	Y
HD 160529	B8-A9	N	N	N		Y
P Cyg	B2	N	**N** [6]	N	spherical	Y
MWC 930	B6	N	**N**	N	spherical	Y
HD 168607	B9	N	**N**	N		
S Dor (LMC)	B3	N	**N**	N	absent?	
Wray 15-751	B0/1	N	Y [7]	N	bipolar	
5 cLBVs						
MWC 314	B + YSg?	Y [8]	Y [8]	Y [9]	large bipolar	Y
HD 168625	B6	N	N	Y [10]	inner loop-like	
Schulte 12	B + NS?	Y [11]	**Y** [11]	Y [12]		Y
Wray 17-96	B[e]	N	N	N	spherical	
Pistol star	B[e]	N	N	Y [13]	spherical	Y

[1] [22]. [2] Spectroscopic monitoring in He I λ10830 line [23]. [3] Wind-collision zone with companion velocity resolved with VLTI-AMBER [24]. [4] Interferometric VLTI, with best orbit or family of orbits [25–27]. [5] Spectroscopic binary indications [11]. [6] Proposed photometric periods of 4.7 y [28], and ∼7 y [29]. [7] Proposed spectroscopic binary without period [11]. [8] This observation program with HERMES [30]. [9] VLT-AO triple hierarchical system [31]. [10] Companion on wide orbit from VLT-AO [31]. [11] This observation program with HERMES [32]. [12] Observed with HST-FGS [33] and speckle obs. [34]. [13] Interferometric companion, remains unconfirmed [35].

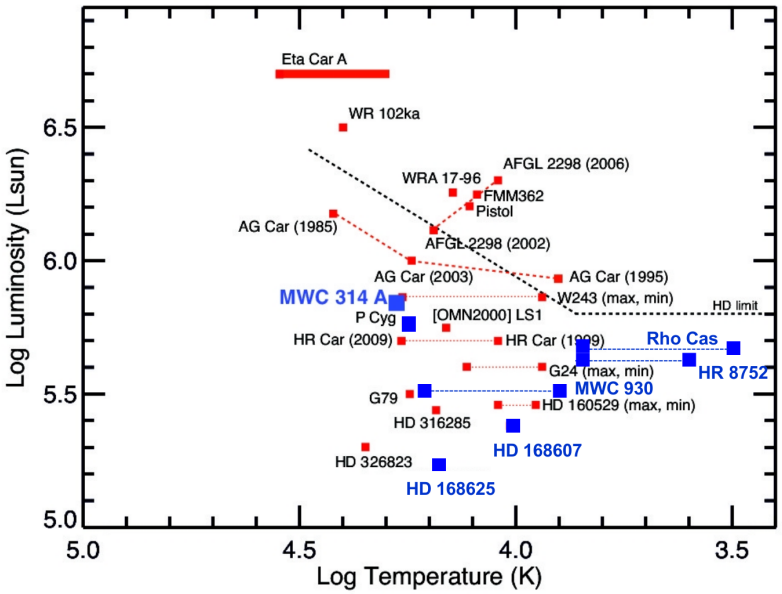


Figure 1. Portion of the upper H-R diagram showing various LBVs and candidate LBVs (boxed symbols). The large boxed symbols are galactic stars we have continuously monitored with high-resolution spectroscopic observations since 2009. The $T_{\rm eff}$ variability of the Yellow Hypergiants ρ Cas and HR 8752, also monitored with HERMES, is also shown (see text).

3. Analysis Methods

For accurate RV determinations using individually selected spectral lines, we have implemented four different automated line measurement methods. First, our computer code searches for anchor points around the lines in wavelength regions of sufficiently constant continuum flux levels for a minimum wavelength interval (e.g., of 0.5 Å). Following the flux normalization, the absorption lines are represented upside-down in groups of four sub-panels per results page. Figure 2 shows an example page where the black solid curved lines are the normalized profiles of Si II, N I, and Fe II lines observed with HERMES. The first RV method straightforwardly determines the velocity position of the line flux minimum marked with the vertical red line. The measured RV values are denoted to the right of this line. They represent the differences in the rest wavelengths in air of the lines placed at 0 km s^{-1} in the barycentric velocity frame. This method is, however, very sensitive to the detailed flux profile inside the line cores. Sometimes, the central cores of weak lines can be bumpy or reveal a double structure that may systematically offset the RV measurements of the lines flux minimum.

We, therefore, also measured line RV values from the bi-sector position at FWHM. They are marked with vertical green lines. The green horizontal broken lines show the total FWHM, and the RV value of their midpoint is denoted to the right. Both methods typically provide similar RV values, although they do tend to deviate more for strongly asymmetric profiles, i.e., due to far violet extended line wings caused by absorption in an accelerating wind. The differences are chiefly sensitive to the excitation energy of the line transition and to the chemical abundances of the line species. For example, the H I Paschen lines are more asymmetric compared to the He I lines, although the latter are often deeper.

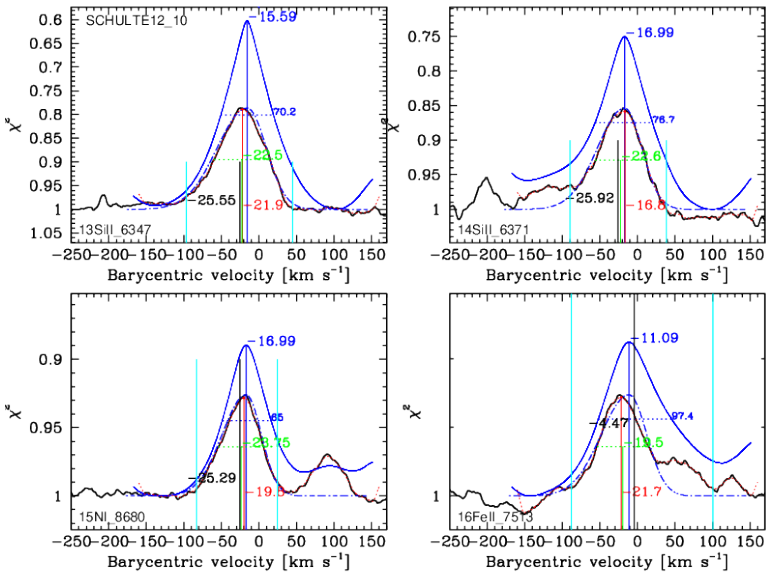


Figure 2. An example of diagnostic graphs we plotted with four radial velocity measurement methods for high-resolution continuum normalized line profiles. The four panels show two Si II lines (**top panels**), a N I line, and an Fe II absorption line (**bottom panels**) observed with HERMES in the cLBV Schulte 12 (see text).

We, therefore, tested and compared two more advanced line RV measurement methods by cross-correlating with a template fit function and by measuring the center of gravity of the entire line profile. The cross-correlation technique first measures the difference between the position of the line flux minimum and the far-red position of the end of the FWHM wavelength interval. This difference is used to calculate the red half of a Gaussian template fit function that matches the observed line depth. The measurement is repeated for the short-wavelength end for adding the blue side to the fit function with the same line depth. This procedure calculates an asymmetric template fit function for each line profile we measure, while being properly adapted to any observed left-to-right line asymmetry. Next, the template is cross-correlated with the observed line profile by calculating the χ^2 differences of the complete line profile (CCF). The calculated line CCFs are shown in blue in Figure 2, where the RV values measured from the CCF minima are also denoted in blue (for the vertical blue lines). The template fit function is overplotted with its minimum placed at the measured RV value (broken blue curves). We typically find good fits to the overall line profiles using the CCF line RV method.

However, we find that the CCF method is rather sensitive to blending with weak lines in the far wings of the main line. This is, for example, shown in the Fe II line (bottom right-hand panel) where the maximum of the fit function (broken blue curve) becomes somewhat shifted towards longer wavelengths compared to the position of the observed line flux minimum (at the vertical red lines). The RV differences with less blended (or unblended) lines remain rather limited ($\sim$5 km s^{-1}), but which can offset our line RV measurements. In most cases, the offsets can be readily detected from the rather flat shapes and large CCF FWHM values compared to those of unblended lines, which typically reveal sharper or more concave CCF shapes. For example, the CCF FWHM value of the Si II and N I lines in Figure 2 is, on average, $\sim$70 km s^{-1}, while we measure $\sim$97 km s^{-1} in the weak Fe II line that is considerably more asymmetric in its long-wavelength wing.

We, therefore, also implemented the line center-of-gravity RV measurement method. It integrates the full line profile between short- and long-wavelength boundaries, which we determine from the steepness of the detailed line wing flux profiles (vertical cyan lines). The center of gravity of the entire line surface area is calculated with respect to the continuum

level (at unity). The RV positions are marked in Figure 2 with the vertical black lines for RV values denoted to the left. We find that the center-of-gravity RV values are typically very consistent (within a few km s^{-1}) between sufficiently unblended lines. We calculated the line RV values using the four methods but give preference to the center-of-gravity method, as it appears to be best suited for handling possible negative effects due to intrinsic line asymmetry, increased noise levels, or apparent line blending with the main absorption lines we select.

We performed automated line RV measurements in a wide variety of absorption and emission lines that we observed in the spectra of Table 1. The line lists used for each c/LBV depend on the spectral type (B3-B9) as the depth of measurable absorption lines is sensitive to $T_{\rm eff}$. The typical SNR values of the spectra are 50–200 but can vary according to the (blue to red) wavelength region of the lines. For example, because Schulte 12 is very extincted towards shorter wavelengths, its typical spectra for 2.5 h of exposure time have sufficient SNR only above 5500 Å but are too noisy below this wavelength. We typically measure the Paschen H I lines; the broad He I and He II lines; ionic metal lines of Si II, Si III, and Si IV; Fe II multiplet lines (i.e., in 4000–4600 Å); high-excitation Ne I lines; the near-IR triplet lines of N I and optical N II and Mg II; and the O I and C II doublet lines. We always tested the temporal stability of our measurements against the RV time series we measured for optical and near-IR Diffuse Interstellar Bands (DIBs). The DIB absorption features reveal very small or no Doppler shifts with time, which also allow us to track the quality of the spectral wavelength calibrations over 15 years.

4. Results

4.1. S Dor

The right-hand panel of Figure 3 shows the V-brightness curve of S Dor we combined from ASAS-3, ESA-Integral OMC, and AAVSO-V observations. It varies by a few tenths of a magnitude on timescales of a few months, superimposed on variations of $\sim 1^{\rm m}.5$ over decades. At minimum brightness, this prototypical LBV reveals prominent metal P Cyg profiles and a spectrum dominated by emission, in particular forbidden Fe II emission lines, but also of helium and a variety of permitted metal lines. At maximum V-brightness, the optical spectrum, however, becomes as cool as an F-type supergiant showing strong ionic metal absorption lines almost free of emission components [36].

To investigate the detailed spectroscopic variability during the dramatic V-variability of S Dor, we compared high-resolution spectra ($R > 50{,}000$) observed between 1997 and 2014 in the wavelength region between 4000 and 7000 Å. The overall spectral variability is characterized by the clear transformation of ionic metal lines from a distinct P Cyg-type profile in 1997 to inverse P Cyg line shapes in 2002–2007. The red-shifted absorption in the inverse P Cyg profiles rapidly weakens in the course of 2008, while the blue-shifted absorption in these wind lines becomes deeper. In 2014, the line profiles resume the strong P Cyg shape observed in 1997, becoming even slightly stronger in certain ionic transitions.

The right-hand panel of Figure 3 shows the detailed profile changes in three Fe II lines observed in February 2007 around maximum V-brightness and in November 2014 during a variability phase where the star's V brightened by $\sim 0^{\rm m}.8$ after a minimum brightness of $V \sim 10^{\rm m}.4$ in 2011. The spectrum of February 2007 around maximum V-brightness indicates $T_{\rm eff} \simeq 8000$ K, while that of November 2014 on the ascending branch signals $T_{\rm eff} \simeq 20$ kK.

The P Cyg-type Fe II line profiles reveal wind expansion velocities of $\sim$200 km/s. The star's RV we measured in the emission flux maxima of weak P Cyg lines was $\simeq$295 km s^{-1}. Note, however, that the inverse P Cyg lines also reveal *red-shifted* velocities of $\sim$150 km s^{-1} with respect to the flux maxima of the central emission line. This signals simultaneous down-flows while the blue-shifted absorption occurs in the wind (hence, with respect to

the star's RV). The emission portions of the composite line profiles reveal constant Doppler positions while the emission line strength (normalized to the local continuum flux level) is strongly variable.

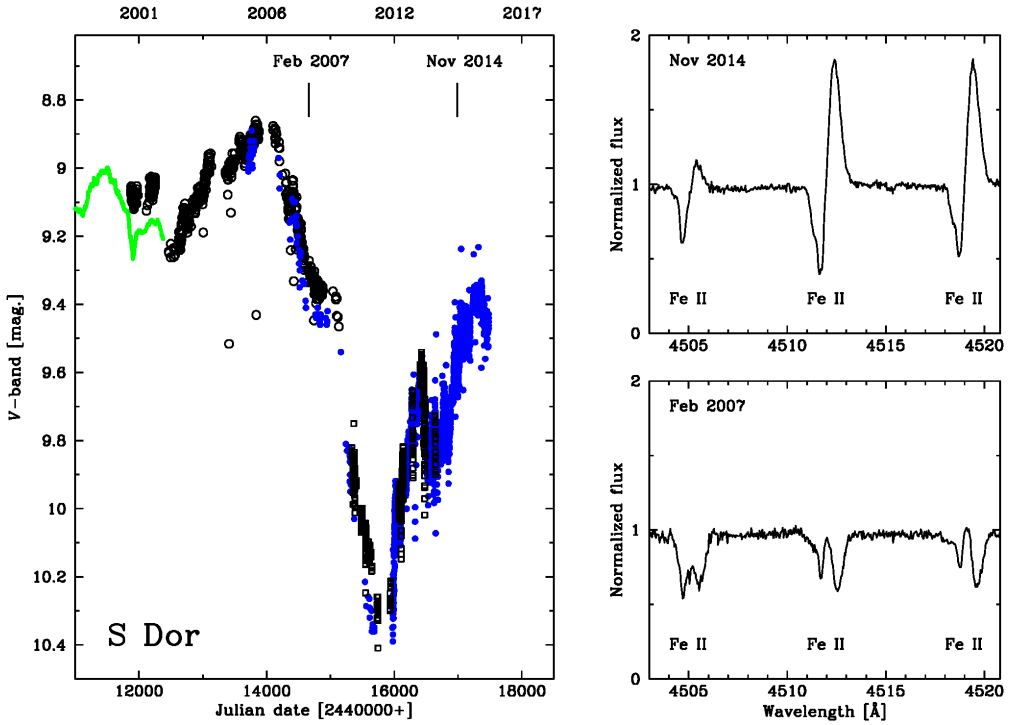


Figure 3. Photometric V-band observations of the LMC LBV S Dor between 2000 and 2015 (**left-hand panel**). The vertical lines mark two high-resolution spectral observations in February 2007 and November 2014 shown in the **right-hand panel** around three Fe II lines. The detailed line profiles transform from inverse (split) P Cyg type in 2007 to strong P Cyg profiles in 2014 (see text).

The high-resolution spectra of S Dor we investigated do not reveal clearly isolated (unblended) absorption lines for unbiased RV measurements. All detailed line shapes between 4000 Å and 4500 Å are combinations of emission lines flanked at either or both sides with absorption lines/features of variable strength and Doppler position that we can attribute to variable wind opacity in the lines' formation region. Notice the double (or split) appearance in the detailed Fe II line profiles of February 2007 when the central line portions reveal emission flux maxima above or below the local continuum level. These remarkably split line shapes are reminiscent of the split profiles that, for example, appeared in the Na D doublet lines of the Yellow Hypergiant ρ Cas (see Figure 3) during a large outburst event in 2000 [37].

For the V-brightness variability of $1^{\mathrm{m}}.2$ observed in 1980–1987, Ref. [38] estimated an $R_\star$ change in S Dor from 100 $R_\odot$ to 380 $R_\odot$, corresponding to T_{eff} = 20 kK to 9 kK when assuming spherical symmetry. The values are provided for the radius of the star itself, not the effective radius of the optically thick wind due to the large mass loss rates. These radius changes would imply small changes in L_* of $\sim$0.2 dex used to expand a small fraction ($<$0.5%) of the stellar mass into the outermost atmospheric layers.

4.2. MWC 930

Ref. [39] identified MWC 930 as a bona fide galactic LBV due to its continued optical and near-IR brightening between 2002 and 2012 (see Figure 4) along with obvious changes in the emission-line spectrum and cooling of the photosphere. Ref. [40] previously investigated the high-resolution optical spectrum and identified P Cyg profiles in selected Fe II lines. The large luminosity of log $L_*/L_\odot$ $\sim$5.5, therefore, signaled the possibility of a cLBV.

Eight spectra of 2000–2004 revealed appreciable changes in the high-excitation Ne I λ6402 line. They were observed while V brightened from $\sim 12^{m}.6$ to $\sim 12^{m}.1$. Ref. [41] discusses the spherical nebula and forbidden metal emission lines observed in the near-IR spectrum of MWC 930.

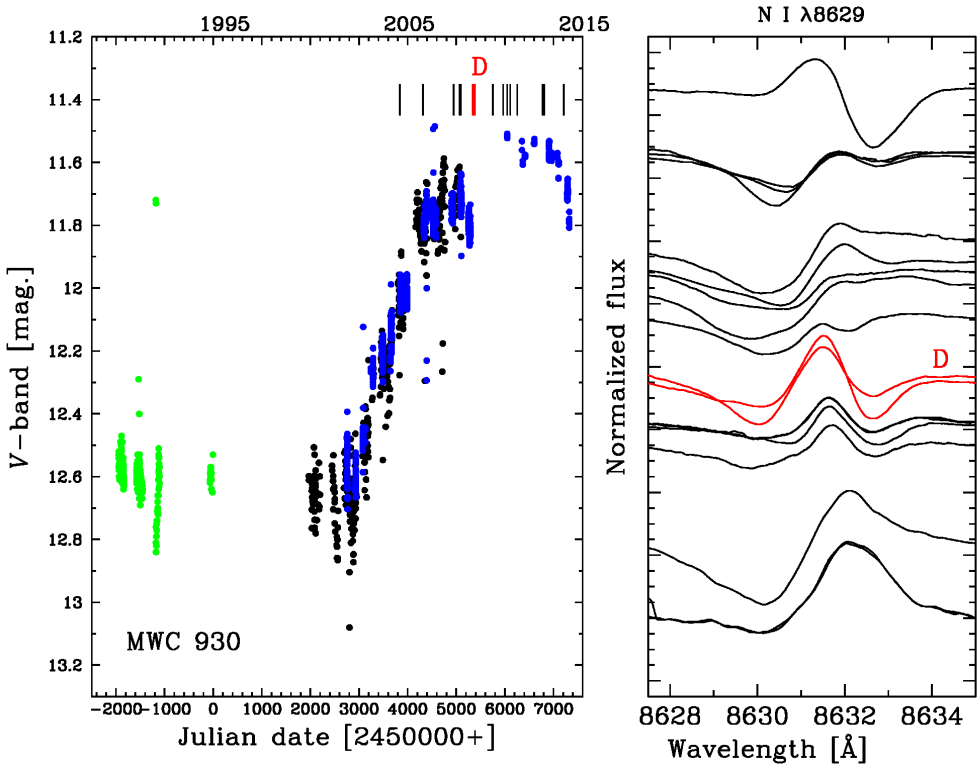


Figure 4. The left-hand panel shows the V-brightness curve of LBV MWC 930 in 1990–2015. The vertical lines mark high-resolution spectroscopic observations. The right-hand panel shows the profile variability in the N I λ8629 line over this period where time runs upwards. Split line profiles (red) are observed in 2010 (D) due to variable central line emission (see text).

The spectroscopic variability of MWC 930 and of S Dor are very similar. In the right-hand panel of Figure 4, we show the high-resolution line profile variability in N I λ8629 from 2006 to 2015 (time runs upward). Similar profile variability is also observed in two other high-excitation ($\sim$10 eV) N I λ7442 and N I λ8629 lines belonging to the same near-IR triplet.

For 2006, the N I lines show prominent P Cyg profiles while MWC 930 brightened to $V \simeq 11^{m}.6$. They reveal wind speeds of $\sim$150 km s^{-1} or the properties of a rather slow wind. For 2009–2015, we observe a remarkable transformation in the line profiles around the maximum V-brightness of 2012. We observe the doubling of the N I absorption line cores developing between 2009 and 2011 (marked in 2010 with D in Figure 4). The long-wavelength absorption portion of the line profiles strengthens while the central core turns in emission assuming maximum flux levels above the local continuum level. During this variability phase, the N I lines are composed of shallow absorption lines on both sides of a narrow strong central emission line. We observe the same profile changes in Fe II lines of S Dor for 2002, well before its large brightness maximum of 2006 (see Figure 4). This transient line-splitting phenomenon is temporarily observed before the V-brightness maximum occurs in both LBVs. The split line profiles disappear after the V-brightness maxima when the central emission lines weaken and the profiles revert to weak but distinctly P Cyg line profiles (i.e., for MWC 930 in 2013 and for S Dor in 2008).

After 2015, we observe a fast V-brightness decrease in MWC 930 while the near-IR N I lines transform into inverse P Cyg profiles. The analysis of high-resolution spectra

and our RV measurements do not demonstrate a spectroscopic binary. The long-term spectroscopic variability of MWC 930 is, in fact, very similar to that of S Dor. An increase of R_* in MWC 930 comparable to S Dor can cause the decrease in $T_{\rm eff}$ to ∼8000 K between 2000 and 2014, resulting in the dramatic line profile variability we observe in the high-resolution spectra.

We think that the development of prominently split absorption line profiles is linked to LBV outbursts with strong V-variability. It results from an instability phase for the LBV atmosphere/wind causing a cyclic, slow expansion and rapid global contraction that produce supersonic (shock wave-like) up- and down-flows in the N I lines' formation region. The line-splitting phenomenon in LBVs is, in fact, very similar to the split metal line cores observed in pulsating cool hypergiants such as the Yellow Hypergiant ρ Cas (F-K Ia$^+$). The line core splitting in LBV MWC 930 is due to an optically thick central emission line produced in the inner ionized wind region that becomes shock-excited with the increase in R_* and the decrease in $T_{\rm eff}$ during the outbursts.

4.3. P Cyg

Figure 5 shows the high-resolution continuum normalized line profiles observed with large SNRs in the LBV P Cyg between Apr 2007 and May 2010. Six spectra are overplotted in the barycentric velocity scale for lines of Balmer Hβ, He I, H Paschen 14, Si III, Al III, and Ne I. The dashed vertical lines mark the center of mass velocity of -8.9 km s^{-1} [42]. It closely corresponds (within ± 5 km s^{-1}) to the Doppler position of the emission maxima of the prominent P Cyg profiles observed in the six lines.

The terminal wind velocity in Balmer Hα is ∼270 km s^{-1} (see Figure 6), while in Hβ, we observe ∼220 km s^{-1}. For the optical and near-IR ionic metal lines, having a higher excitation energy ($\chi_{\rm low}$), the absorption portions of the P Cyg profiles are considerably weaker, also showing smaller wind velocities ranging from ∼50 km s^{-1} to 200 km s^{-1}. The V-brightness curve for 2008–2010 in Figure 6 shows rather irregular variability between $5^{\rm m}.0$ and $4^{\rm m}.6$. The variability of the violet absorption wing in Hα above ∼230 km s^{-1} corresponds to moderate V-variability of $0^{\rm m}.1$ to $0^{\rm m}.2$ for ∼4 m in 2009.

The spectral variability in the high-excitation lines such as Ne I λ6402 is caused by the variable opacity at the base of the supersonic wind in P Cygni. These weak ionic lines, including Si III and Al III, form close to the stellar photosphere and demonstrate the variability of the wind base for velocities well below 200 km s^{-1}. Remarkably, during certain variability phases, the emission portion of weak P Cyg lines can vanish (i.e., in Si III in November 2007). For example, we observe wind absorption in the H I Pa14 and Ne I lines, which considerably varies over a period of only about ∼1 m (black and red drawn spectra of May and June 2009).

We have investigated the RV time series of selected optical and near-IR lines in the high-resolution spectra of LBV P Cygni but have not detect clear indications of periodic variability so far. The spectral lines we can measure are typically combinations of absorption and emission lines blending together, very similar to the composite line shapes we observe in S Dor and MWC 930. The high-resolution profiles in the absorption portions of weak P Cyg lines vary irregularly over time with the variability of V. They, however, do not reveal clear signatures of any strictly periodic variability that we can attribute to orbital motion.

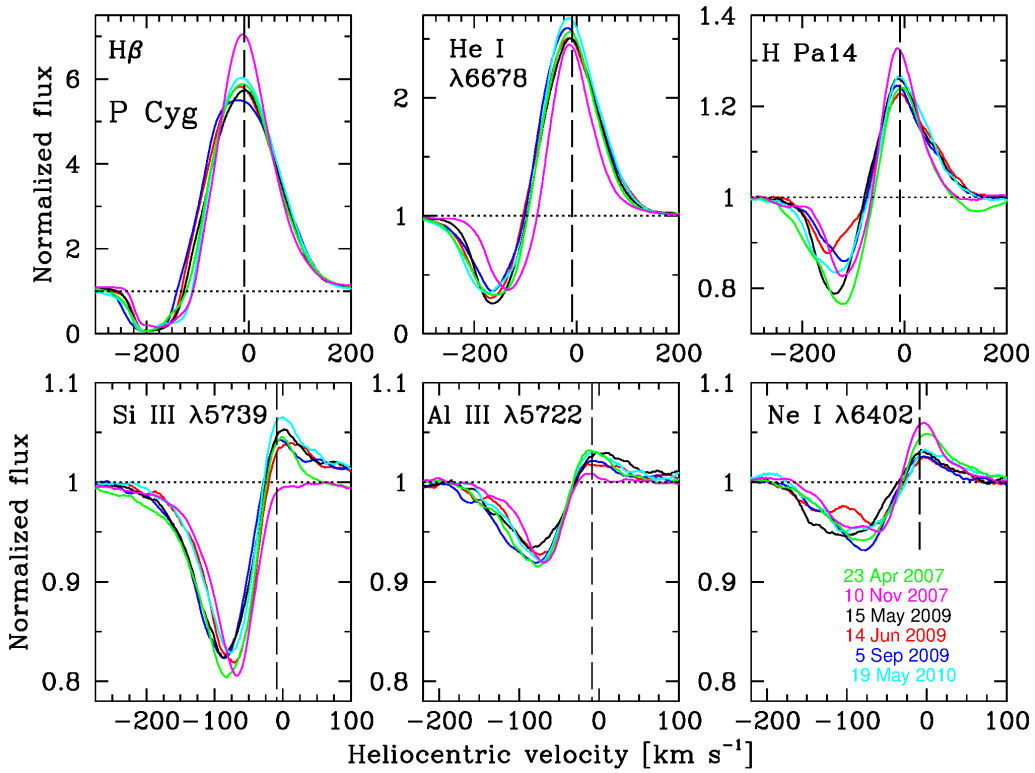


Figure 5. Selection of 6 lines in the optical and near-IR high-resolution spectra of P Cygni observed with large SNRs between April 2007 and May 2010. The variable absorption in the line profiles is caused by variable wind opacity (see text).

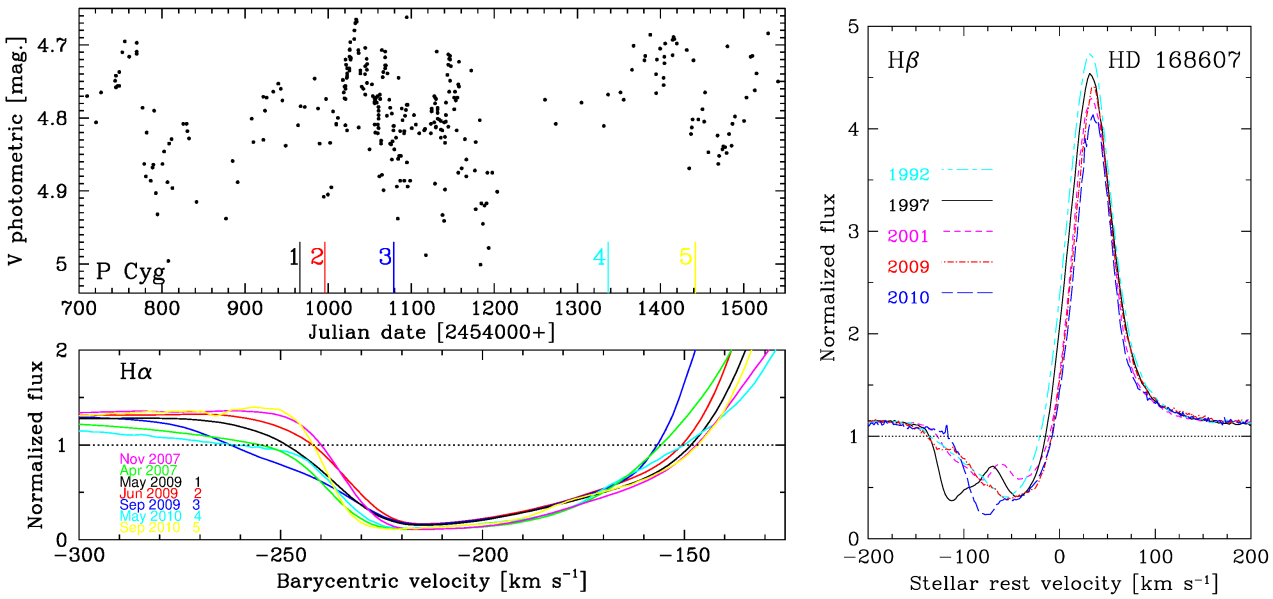


Figure 6. The left-hand top panel shows *V*-brightness observations of P Cygni in 2008–2010, where the vertical lines mark high-resolution spectroscopic observations (1–5). The changes in Hα absorption are caused by wind variability shown for 7 color-coded spectra of 2007–2010 (left-hand bottom panel). The right-hand panel shows migrating DACs in Hβ of LBV HD 168607 observed in 1992–2010.

4.4. HD 168607

The left-hand panel of Figure 7 shows five high-resolution spectra of HD 168607 observed in 1997–2010 (time runs upwards) in four Fe II lines around 4515 Å. The lines show the strong LBV variability in the detailed profiles, very similar to S Dor and P Cyg. For 1997,

the Fe II lines reveal split core profiles transforming into strong emission lines in 2001, which we also observe in S Dor and MWC 930 (see Sections 4.1 and 4.2). Note that unlike these LBVs, there are currently no indications of a circumstellar nebula in HD 168607 [31].

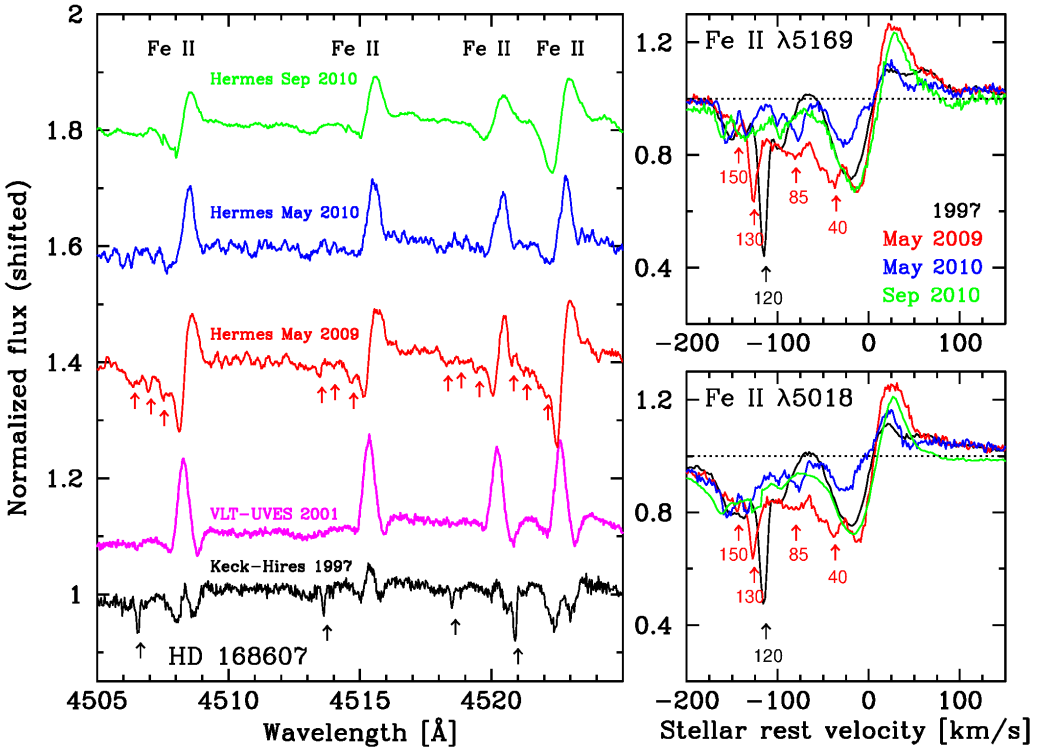


Figure 7. The left-hand panel shows strong variability in high-resolution profiles of 4 Fe II lines of the LBV HD 168607 in 1997–2010. We observe DACs in 1997 and 2009 marked with arrow symbols. The right-hand panels show two Fe II multiplet lines in the stellar rest frame with the velocities of 5 DACs denoted at the arrow symbols (see text).

We find that the depths of the absorption portion of the Fe II P Cyg profiles are strongly variable with time. However, in the spectra of 1997 and 2009, we observe Discrete Absorption Components (DACs), which we mark with arrow symbols. The DACs signal the development of large-scale dynamic structures in the LBV's supersonic wind. Migrating DACs are, for example, also observed in the UV spectra of less luminous B-supergiants such as J Pup (HD 64760) [43].

We observe the migrating DACs in strong P Cyg profiles of Hβ (see Figure 7), which were also studied by [44]. They are observed in this line around wind velocities of 60 km s^{-1} to 120 km s^{-1}. The right-hand panels of Figure 7 show the detailed profiles of the Fe II λ5169 (top panel) and Fe II λ5018 (bottom panel) lines that belong to the same optical multiplet. The profile variability is shown for four observations in 1997–2010. In May 2009, four DACs were observed at 40, 85, 130, and 150 km s^{-1} in the stellar rest frame (red lines). It is important to point out that the DACs are observed in Fe II lines that share the same multiplet; and therefore, the features can not be confused with sharp Earth lines or increased noise levels. This is also the case for the sharp and deep DAC we detected at 120 km s^{-1} in the Fe II lines of 1997 (black lines). In May and September 2010 (blue and green lines), we also observed DACs that were, however, weaker compared to 1997 and 2009.

We searched for periodicity in the RV time series of lines we selected in the optical and near-IR high-resolution spectra of HD 168607. While the Mg II λ4481 and Si II λ6347 lines appear in absorption, the Hα line shows a strong P Cyg profile; also, the He I lines, such as λ4471, are often partially filled in with emission, which can offset the RV measurements.

4.5. Schulte 12

As an X-ray source, the cLBV Schulte 12 in the Cyg OB2 association is a good candidate for binarity because single B-stars are not sufficiently hot to produce X-rays by themselves. A few sources in the literature have reported on its RV variations; however, the small sizes of the studied samples prevent any meaningful search for periodicity.

So far, we have observed 28 high-resolution HERMES spectra. They were combined with 24 archive spectra from the 3.5-m Calar Alto telescope in Spain. The left-hand and middle panels of Figure 8 show four lines of three HERMES spectra observed in 2012–2024. The right-hand panels show the stability of two DIBs compared to the four lines. The latter lines are clearly variable in both Doppler velocity and shape over the 12 years.

We measured the center-of-gravity RV values for a couple of dozen lines. Our periodogram analysis of the RV time series reveals a significant signal around ∼33 d, consistent with previously published high-precision photometric observations. By attributing the ∼33 d period to orbital motion, we also calculated orbital parameters, including the mass ratio. In the case where we adopted a typical LBV primary mass of 50–100 $M_{\odot}$, it yielded a companion mass of 1–2 $M_{\odot}$.

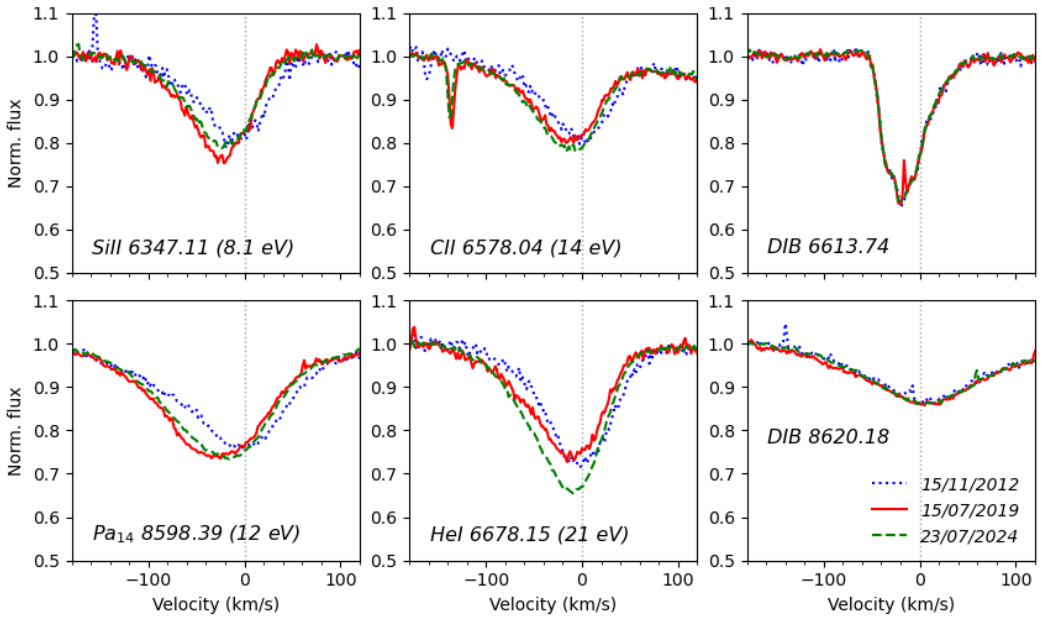


Figure 8. The high-resolution profiles of 4 lines (with their lower energy levels) observed in 3 spectra of 2012–2024 are shown in the left-hand and middle panels in the barycentric velocity frame. The lines' Doppler shift over time, also showing detailed profile variability. The velocity positions and shapes of two DIBs are invariable, as shown in the right-hand panels. The narrow features are Earth lines or noise spikes.

The line profile variability in the metal lines and the Balmer Hα line of Schulte 12 are nearly identical to the line variability observed in various high-mass X-ray binaries having a compact companion (such as Vela X-1). We propose that Schulte 12 is an active binary system consisting of a B-supergiant transferring mass to a compact object, likely a neutron star. This would provide a proper explanation for the X-ray fluxes from Schulte 12. We think they originate in accretion structures around a relativistic companion star. Note, however, that the question of if Schulte 12 belongs to the special class of c/LBVs is still a matter of debate. If it does, this remarkable object would be the first known pair of a cLBV and a neutron star. A journal paper on this research is currently in preparation [32].

5. Discussion and Conclusions

Table 2 provides a compilation of the 10 LBVs and 5 cLBVs we investigated for the literature references proposing/confirming (or rejecting) the spectroscopic binarity (column 4) of these stars. Column 5 also lists published binary detections using imaging/interferometric methods. Only LBVs η Car and HR Car are spectroscopic binaries with published orbital elements. Seven other LBVs in Table 2 are not spectroscopic binaries despite various long-term spectroscopic studies. HD 160529 is discussed in [11,45]. Ref. [46] reports indications of binarity in Wd-1 243, although Ref. [11] does not confirm it. Many references speculate on the possible binarity of LBV AG Car, but direct evidence from spectroscopy or imaging has so far not been provided.

Wray15-751 is an interesting new case of a candidate spectroscopic binary proposed by [11] based on line RV measurements in 10 spectra. V strongly brightens in 1990–2011 (similar to S Dor and MWC 930), followed by a steep dimming typical of an S Dor cycle. More spectroscopic monitoring is urgently needed to confirm the proposed binarity.

For the three LBVs P Cyg, MWC 930, and HD 168607 in Table 2, we do not find evidence of spectroscopic binaries despite our ∼15 y monitoring campaign with HERMES. A search for periodicity in the RV curves does not reveal strict periodicity in any of the spectral lines we selected. We find, however, that the RV periodograms are rather sensitive to the properties of the selected lines. Optical and near-IR lines in LBVs are almost always contaminated by emission contributions in the lines (e.g., S Dor in Figure 2). The emission line portion above the continuum level may even vanish, although the absorption portion stays filled in by the emission, which can offset the line RV measurements. Only a few weak lines can be reliably measured in the three LBVs, although we do not find clear evidence of periodicity. Note that only for P Cygni have two periods of 4.7 y and ∼7 y in photometric time series been proposed (see footnotes in Table 2).

Our high-resolution monitoring of cLBV MWC 314, on the other hand, does reveal a single period of 60.8 d [30]. Note that [31] detected a wide companion in MWC 314, which is, therefore, also a triple hierarchical system. We find that the HERMES monitoring of Schulte 12 also reveals a clear ∼33 d signal in the RV periodograms of selected lines (see Section 4.5). The companion of η Car is a massive O/W-R star [47], while for HR Car, a red supergiant companion has been proposed [27]. The companion of cLBV MWC 314, having well-established orbital parameters [30], could be a yellow supergiant, but this also requires confirmation.

Spectroscopic time-series studies of the LBVs Wd-1 243, AG Car, and HD 160529 (and also S Dor, which we investigated with five spectra as detailed in Section 4.1) do not show evidence of binarity. This prompts the question of why clear spectroscopic signatures of orbital motion in very massive hot stars are so elusive. Can the strong LBV wind variability completely mask their orbital motions, or are these LBVs *single* massive stars after all? Can this problem be addressed with long-term spectroscopic monitoring campaigns only? This also appears to be at odds with the detection of X-rays in Wd-1 243, AG Car, HD 160529, P Cyg, and MWC 930 (Table 2). We may assume that X-rays, in fact, originate from binary component interactions with the supersonic LBV wind. How are the non-spherical nebula of AG Car and the spherical nebula of MWC 930 then formed? Both LBVs showed prominent S Dor cycles over the last two decades (together with the associated spectral variability we observe), which requires an efficient mass ejection mechanism in these LBVs.

Ref. [8] recently discussed strong expansion effects observed in 3D hydro-simulations in the envelopes of single massive star models, reminiscent of S Dor cycles. Their simulations do not rule out binary interactions for producing the S Dor-type outbursts, but they neither exclude an efficient driving mechanism for the global eruptions of the envelope of a *single* massive star. As a proof of concept, Ref. [48] calculated stellar evolution models that

include wind–envelope interactions where the envelope contraction is triggered by mass loss variations, creating a feedback loop between the wind and the envelope structure that lacks a stable equilibrium, thus enabling cyclic behavior on the thermal time scale of the inflated envelope. Currently, simulating full S Dor cycles in 3D is beyond the state of the art due to computational costs and the complexity of incorporating all relevant 3D effects; there are plausible physical arguments suggesting that mechanisms other than wind–envelope interactions, such as radiative cooling or changes in continuum opacity, could facilitate the contraction phase after expansion, a notion that requires validation through more advanced and computationally intensive 3D hydro-simulations in the future. We also note that well-known Yellow Hypergiants, such as ρ Cas, show recurring outbursts every $\sim$10 to 40 y (see Figure 1), although no signatures of binarity have been observed to date. YHGs show pulsation-induced outburst events when the atmosphere globally expands by a factor of $\sim$2, thereby cooling with $\sim$3000 K over time scales of typically 1-2 y [37,49].

We also find evidence that fast LBV winds contain large-scale dynamic structures because we observe migrating DACs in the HERMES spectra of HD 168607 (Section 4.4). DACs are observed at velocities of 40–150 km s^{-1} in Fe II P Cyg lines, and also in the broad Balmer Hβ line (see Figures 6 and 7). The DACs are caused by streams or "Corotating Interaction Regions" (abbreviated CIRs; [50]). These are large-scale wind velocity perturbations (or "density–velocity spirals") due to the radiative driving of a rotating wind. They are mainly studied in the ultraviolet (IUE) spectra of less-luminous (Ib) B-supergiants and O-stars [51]. For example, we have also observed DACs in the cLBV MWC 314, a confirmed binary system [52,53].

A detailed multi-D radiative transfer modeling of accelerating DACs [43] shows that they form behind the CIRs, while the DAC line formation region with the rotation moves away from the stellar surface, causing them to accelerate through the lines. The CIRs can form above bright (noncorotating) surface spots that differentially accelerate the wind outflow. However, the origin of the rotating bright spots is still unclear, although they could result from the superposition of pro- or retrograde propagating mechanical waves near the base of the equatorial wind (i.e., Rossby waves). Remarkably, we also observe these migrating DACs in the winds of the more massive LBVs. More work is needed to model the DACs of LBVs as they may provide important new information on the strongly variable wind dynamics of LBVs.

Our investigation of 10 LBVs and 5 cLBVs (summarized in Table 2) shows that evidence for binary interactions as the primary cause of S Dor cycles remains inconclusive, and it is possibly not needed. While we have detected a periodic RV signal in cLBV Schulte 12 for the first time, so far, we have not found clear periodic RV signals for the LBVs MWC 930, P Cyg, and HD 168607. This lack of consistent periodicity across multiple LBVs suggests that binary interactions are not the sole or primary driver of the S Dor cycles. In fact, only Eta Car and HR Car (Wray 15-751 is a candidate) out of 10 LBVs, and MWC 314 and Schulte 12 out of 5 cLBVs in Table 2, appear to be spectroscopic binaries.

Instead, our results lend support to the hypothesis that internal instability mechanisms within LBVs play an important role for triggering S Dor cycles. Notably, S Dor and MWC 930 have shown clear S Dor cycles during our 15-year spectroscopic monitoring program, despite the absence of periodic RV signals that would indicate binary systems. While binary interactions such as those observed in Eta Car can lead to mass transfer and tidal effects (that may trigger giant outbursts), the lack of consistent evidence for binarity in our RV measurements so far suggests that envelope instabilities in single stars could be a primary driver of the S Dor cycles. The new detection of Discrete Absorption Components in LBV HD 168607, indicative of large-scale structures in a rotating wind, also further supports the importance of intrinsic stellar processes in LBV variability.

Author Contributions: Conceptualization, methodology, software, validation, formal analysis, investigation, visualization, writing—review and editing, A.L. and N.G.; resources, data curation, supervision, project administration, funding acquisition, A.L. All authors have read and agreed to the published version of the manuscript.

Funding: A.L. acknowledges in part funding from the European Union's Framework Programme for Research and Innovation Horizon 2020 (2014–2020) under the Marie Skłodowska-Curie grant Agreement No. 823734: Physics of Extreme Massive Stars (EC-POEMS). N.G. acknowledges support by a Belgian Federal government grant for Ukrainian post-doctoral researchers (contract UF/2022/10).

Data Availability Statement: The datasets presented in this article are not readily available because they are part of an ongoing long-term monitoring program. Requests to access the datasets should be directed to the corresponding author.

Acknowledgments: We thank the anonymous referees for their valuable comments. A.L. thanks the Belgian Federal Science Policy Office (BELSPO) for their support in the framework of the PRODEX Programme. The Mercator telescope is operated by the Flemish Community on the island of La Palma at the Spain Observatory del Roche de los Muchachos of the Instituto de Astrofisica de Canarias. Mercator and HERMES are supported by the Funds for Scientific Research of Flanders (FWO), the Research Council of KU Leuven, the Fonds National de la Recherche Scientifique (FNRS), the Royal Observatory of Belgium, the Observatoire de Genève, and the Thüringer Landessternwarte Tautenburg. We thank all observers who collected data for this long-term HERMES monitoring program. This research made use of the NASA Astrophysics Data System.

Conflicts of Interest: The authors declare no conflicts of interest.

References

1. Humphreys, R.M.; Davidson, K. The Luminous Blue Variables: Astrophysical Geysers. *Publ. Astron. Soc. Pac.* **1994**, *106*, 1025. [CrossRef]
2. Davidson, K.; Humphreys, R.M. (Eds.) *Eta Carinae and the Supernova Impostors*; Astrophysics and Space Science Library; Springer: New York, NY, USA, 2012; Volume 384. [CrossRef]
3. Humphreys, R.M.; Weis, K.; Davidson, K.; Gordon, M.S. On the Social Traits of Luminous Blue Variables. *Astrophys. J. ApJ* **2016**, *825*, 64. [CrossRef]
4. van Genderen, A.M. S Doradus variables in the Galaxy and the Magellanic Clouds. *Astron. Astrophys. A&A* **2001**, *366*, 508–531. [CrossRef]
5. van Genderen, A.M. Further VBLUW photometry of the S DOR type variables S DOR and HDE 269006 in the LMC and a discussion on their temperatures. *Astron. Astrophys. A&A* **1982**, *112*, 61–67.
6. Conti, P.S. Basic Observational Constraints on the Evolution of Massive Stars. *IAU Symp.* **1984**, *105*, 233.
7. Boffin, H.M.J.; Beccari, G.; Petr-Gotzens, M.G. Report on the ESO Workshop "The Impact of Binaries on Stellar Evolution". *Messenger* **2017**, *169*, 61–64. [CrossRef]
8. Jiang, Y.F.; Cantiello, M.; Bildsten, L.; Quataert, E.; Blaes, O.; Stone, J. Outbursts of luminous blue variable stars from variations in the helium opacity. *Nature* **2018**, *561*, 498–501. [CrossRef]
9. Langer, N.; García-Segura, G.; Mac Low, M.M. Giant Outbursts of Luminous Blue Variables and the Formation of the Homunculus Nebula around η Carinae. *Astrophys. J. ApJ* **1999**, *520*, L49–L53. [CrossRef]
10. Podsiadlowski, P.; Joss, P.C.; Hsu, J.J.L. Presupernova Evolution in Massive Interacting Binaries. *Astrophys. J. ApJ* **1992**, *391*, 246. [CrossRef]
11. Mahy, L.; Lanthermann, C.; Hutsemékers, D.; Kluska, J.; Lobel, A.; Manick, R.; Miszalski, B.; Reggiani, M.; Sana, H.; Gosset, E. Multiplicity of Galactic luminous blue variable stars. *Astron. Astrophys. A&A* **2022**, *657*, A4. [CrossRef]
12. Moe, M.; Di Stefano, R. Mind Your Ps and Qs: The Interrelation between Period (P) and Mass-ratio (Q) Distributions of Binary Stars. *Astrophys. J. ApJS* **2017**, *230*, 15. [CrossRef]
13. Banyard, G.; Sana, H.; Mahy, L.; Bodensteiner, J.; Villaseñor, J.I.; Evans, C.J. The observed multiplicity properties of B-type stars in the Galactic young open cluster NGC 6231. *Astron. Astrophys. A&A* **2022**, *658*, A69. [CrossRef]
14. Bodensteiner, J.; Sana, H.; Wang, C.; Langer, N.; Mahy, L.; Banyard, G.; de Koter, A.; de Mink, S.E.; Evans, C.J.; Götberg, Y.; et al. The young massive SMC cluster NGC 330 seen by MUSE. II. Multiplicity properties of the massive-star population. *Astron. Astrophys. A&A* **2021**, *652*, A70. [CrossRef]

15. Dsilva, K.; Shenar, T.; Sana, H.; Marchant, P. A spectroscopic multiplicity survey of Galactic Wolf-Rayet stars. I. The northern WC sequence. *Astron. Astrophys. A&A* **2020**, *641*, A26. [CrossRef]
16. Neugent, K.F.; Levesque, E.M.; Massey, P.; Morrell, N.I.; Drout, M.R. The Red Supergiant Binary Fraction of the Large Magellanic Cloud. *Astrophys. J. ApJ* **2020**, *900*, 118. [CrossRef]
17. van Genderen, A.M.; de Groot, M.; Sterken, C. New perceptions on the S Doradus phenomenon and the micro variations of five Luminous Blue Variables (LBVs). *Astron. Astrophys. A&AS* **1997**, *124*, 517–531. [CrossRef]
18. van Genderen, A.M.; Sterken, C.; de Groot, M. New discoveries on the S DOR phenomenon based on an investigation of the photometric history of the variables AG Car, S Dor and η Car. *Astron. Astrophys. A&A* **1997**, *318*, 81–98.
19. Raskin, G.; van Winckel, H.; Hensberge, H.; Jorissen, A.; Lehmann, H.; Waelkens, C.; Avila, G.; de Cuyper, J.P.; Degroote, P.; Dubosson, R.; et al. HERMES: A high-resolution fibre-fed spectrograph for the Mercator telescope. *Astron. Astrophys. A&A* **2011**, *526*, A69. [CrossRef]
20. Clark, J.S.; Najarro, F.; Negueruela, I.; Ritchie, B.W.; Urbaneja, M.A.; Howarth, I.D. On the nature of the galactic early-B hypergiants. *Astron. Astrophys. A&A* **2012**, *541*, A145. [CrossRef]
21. Klochkova, V.G.; Islentieva, E.S.; Panchuk, V.E. On the Status of the Star Schulte 12 in the Association Cyg OB2. *Astron. Rep.* **2022**, *66*, 998–1007.
22. Damineli, A.; Hillier, D.J.; Corcoran, M.F.; Stahl, O.; Levenhagen, R.S.; Leister, N.V.; Groh, J.H.; Teodoro, M.; Albacete Colombo, J.F.; Gonzalez, F.; et al. The periodicity of the η Carinae events. *Mon. Not. R. Astron. Soc. MNRAS* **2008**, *384*, 1649–1656.
23. Damineli, A. The 5.52 Year Cycle of Eta Carinae. *Astrophys. J. ApJ* **1996**, *460*, L49. [CrossRef]
24. Weigelt, G.; Hofmann, K.H.; Schertl, D.; Clementel, N.; Corcoran, M.F.; Damineli, A.; de Wit, W.J.; Grellmann, R.; Groh, J.; Guieu, S.; et al. VLTI-AMBER velocity-resolved aperture-synthesis imaging of η Carinae with a spectral resolution of 12 000. Studies of the primary star wind and innermost wind-wind collision zone. *Astron. Astrophys. A&A* **2016**, *594*, A106.
25. Rivinius, T.; Boffin, H.M.J.; de Wit, W.J.; Mehner, A.; Martayan, C.; Guieu, S.; Le Bouquin, J.B. Binarity of the LBV HR Car. In *Proceedings of the International Astronomical Union*; IAU Symposium; Meynet, G., Georgy, C., Groh, J., Stee, P., Eds.; Cambridge University Press: Cambridge, UK, 2015; Volume 307, pp. 295–296.
26. Boffin, H.M.J. An interferometric view of binary stars. In Proceedings of the Optical and Infrared Interferometry and Imaging V, Edinburgh, UK, 26 June–1 July 2016; Volume 9907, p. 99073.
27. Boffin, H.M.J.; Rivinius, T.; Mérand, A.; Mehner, A.; LeBouquin, J.B.; Pourbaix, D.; de Wit, W.J.; Martayan, C.; Guieu, S. The luminous blue variable HR Carinae has a partner. Discovery of a companion with the VLTI. *Astron. Astrophys. A&A* **2016**, *593*, A90.
28. Michaelis, A.M.; Kashi, A.; Kochiashvili, N. Periodicity in the light curve of P Cygni-Indication for a binary companion? *N. Astron.* **2018**, *65*, 29–34.
29. Kashi, A. An indication for the binarity of P Cygni from its 17th century eruption. *Mon. Not. R. Astron. Soc. MNRAS* **2010**, *405*, 1924–1929.
30. Lobel, A.; Groh, J.H.; Martayan, C.; Frémat, Y.; Torres Dozinel, K.; Raskin, G.; Van Winckel, H.; Prins, S.; Pessemier, W.; Waelkens, C.; et al. Modelling the asymmetric wind of the luminous blue variable binary MWC 314. *Astron. Astrophys. A&A* **2013**, *559*, A16.
31. Martayan, C.; Lobel, A.; Baade, D.; Mehner, A.; Rivinius, T.; Boffin, H.M.J.; Girard, J.; Mawet, D.; Montagnier, G.; Blomme, R.; et al. Luminous blue variables: An imaging perspective on their binarity and near environment. *Astron. Astrophys. A&A* **2016**, *587*, A115.
32. Gorlova, N.; Lobel, A. Binarity of cLBV Cyg OB2 #12. *Astron. Astrophys. A&A* 2025, *in press.*
33. Caballero-Nieves, S.M.; Nelan, E.P.; Gies, D.R.; Wallace, D.J.; DeGioia-Eastwood, K.; Herrero, A.; Jao, W.C.; Mason, B.D.; Massey, P.; Moffat, A.F.J.; et al. A High Angular Resolution Survey of Massive Stars in Cygnus OB2: Results from the Hubble Space Telescope Fine Guidance Sensors. *Astron. J. AJ* **2014**, *147*, 40.
34. Maryeva, O.V.; Chentsov, E.L.; Goranskij, V.P.; Dyachenko, V.V.; Karpov, S.V.; Malogolovets, E.V.; Rastegaev, D.A. On the nature of high reddening of Cygnus OB2 #12 hypergiant. *Mon. Not. R. Astron. Soc. MNRAS* **2016**, *458*, 491–507.
35. Martayan, C.; Lobel, A.; Baade, D.; Blomme, R.; Frémat, Y.; LeBouquin, J.B.; Selman, F.; Girard, J.; Mérand, A.; Montagnier, G.; et al. On the Binarity of LBV Stars. In Proceedings of the Joint ESP/Brazilian Workshop, Foz do Iguacu, Brazil, 27 February–2 March 2012; Astronomical Society of the Pacific: San Francisco, CA, USA, 2012; Volume 464, p. 293.
36. Massey, P. An Unprecedented Change in the Spectrum of S Doradus: As Cool as It Gets. *Publ. Astron. Soc. Pac.* **2000**, *112*, 144–147. [CrossRef]
37. Lobel, A.; Dupree, A.K.; Stefanik, R.P.; Torres, G.; Israelian, G.; Morrison, N.; de Jager, C.; Nieuwenhuijzen, H.; Ilyin, I.; Musaev, F. High-Resolution Spectroscopy of the Yellow Hypergiant ρ Cassiopeiae from 1993 through the Outburst of 2000–2001. *Astrophys. J. ApJ* **2003**, *583*, 923–954.
38. Lamers, H.J.G.L.M. Observations and Interpretation of Luminous Blue Variables. In *IAU Colloq. 155: Astrophysical Applications of Stellar Pulsation*; Stobie, R.S., Whitelock, P.A., Eds.; Astronomical Society of the Pacific Conference Series; Astronomical Society of the Pacific: San Francisco, CA, USA, 1995; Volume 83, p. 176.

39. Miroshnichenko, A.S.; Manset, N.; Zharikov, S.V.; Zsargo, J.; Juarez Jimenez, J.A.; Groh, J.H.; Levato, H.; Grosso, M.; Rudy, R.J.; Laag, E.A.; et al. Confirmation of the luminous blue variable status of MWC 930. *Adv. Astron.* **2014**, *2014*, E7
40. Miroshnichenko, A.S.; Bjorkman, K.S.; Grosso, M.; Levato, H.; Grankin, K.N.; Rudy, R.J.; Lynch, D.K.; Mazuk, S.; Puetter, R.C. MWC 930—A new luminous blue variable candidate. *Mon. Not. R. Astron. Soc. MNRAS* **2005**, *364*, 335–343. [CrossRef]
41. Cerrigone, L.; Umana, G.; Buemi, C.S.; Hora, J.L.; Trigilio, C.; Leto, P.; Hart, A. Spitzer observations of a circumstellar nebula around the candidate luminous blue variable MWC 930. *Astron. Astrophys. A&A* **2014**, *562*, A93.
42. Gontcharov, G.A. Pulkovo Compilation of Radial Velocities for 35 495 Hipparcos stars in a common system. *Astron. Lett.* **2006**, *32*, 759–771.
43. Lobel, A.; Blomme, R. Modeling Ultraviolet Wind Line Variability in Massive Hot Stars. *Astrophys. J. ApJ* **2008**, *678*, 408–430.
44. Chentsov, E.L.; Gorda, E.S. Spatial Closeness of the White Hypergiants HD 168607 and HD 168625. *Astron. Lett.* **2004**, *30*, 461–468. [CrossRef]
45. Stahl, O.; Gäng, T.; Sterken, C.; Kaufer, A.; Rivinius, T.; Szeifert, T.; Wolf, B. Long-term spectroscopic monitoring of the Luminous Blue Variable HD 160529. *Astron. Astrophys. A&A* **2003**, *400*, 279–291.
46. Ritchie, B.W.; Clark, J.S.; Negueruela, I.; Najarro, F. Spectroscopic monitoring of the luminous blue variable Westerlund1-243 from 2002 to 2009. *Astron. Astrophys. A&A* **2009**, *507*, 1597–1611.
47. Iping, R.C.; Sonneborn, G.; Gull, T.R.; Massa, D.L.; Hillier, D.J. Detection of a Hot Binary Companion of η Carinae. *Astrophys. J. ApJ* **2005**, *633*, L37–L40.
48. Grassitelli, L.; Langer, N.; Mackey, J.; Gräfener, G.; Grin, N.J.; Sander, A.A.C.; Vink, J.S. Wind-envelope interaction as the origin of the slow cyclic brightness variations of luminous blue variables. *Astron. Astrophys. A&A* **2021**, *647*, A99.
49. van Genderen, A.M.; Lobel, A.; Timmerman, R.; Deul, E.R.; Vos, A.; Nieuwenhuijzen, H.; van Ballegoij, E.J.; Sblewski, M.; Henry, G.W.; Blown, E.; et al. Investigation of the pulsations, outbursts, and evolution of the yellow hypergiants: ρ Cas, HR 8752, and HR 5171A, with notes on HD 179821. *Astron. Astrophys. A&A* **2025**, *694*, A136. [CrossRef]
50. Owocki, S.P.; Cranmer, S.R.; Fullerton, A.W. Periodic Variations in Ultraviolet Spectral Lines of the B0.5 Ib Star HD 64760: Evidence for Corotating Wind Streams Rooted in Surface Variations. *Astrophys. J. ApJ* **1995**, *453*, L37. [CrossRef]
51. Cranmer, S.R.; Owocki, S.P. Hydrodynamical Simulations of Corotating Interaction Regions and Discrete Absorption Components in Rotating O-Star Winds. *Astrophys. J. ApJ* **1996**, *462*, 469.
52. Lobel, A.; Martayan, C.; Mehner, A.; Groh, J.H. Modeling and Observations of Massive Binaries with the B[e] Phenomenon. In *The B[e] Phenomenon: Forty Years of Studies*; Astronomical Society of the Pacific Conference Series; Miroshnichenko, A., Zharikov, S., Korčáková, D., Wolf, M., Eds.; Astronomical Society of the Pacific: San Francisco, CA, USA, 2017; Volume 508, p. 245. Available online: http://aspbooks.org/a/volumes/article_details/?paper_id=38008 (accessed on 26 March 2025).
53. Lobel, A.; Martayan, C.; Baade, D.; Mehner, A.; Groh, J.H. Imaging and Spectroscopy of The Massive Binaries MWC 314 and HD 168625. In *The Physics of Evolved Stars: A Conference Dedicated to the Memory of Olivier Chesneau*; EAS Publications Series; EAS: Pasadena, CA, USA, 2015; Volume 71–72, pp. 169–171. [CrossRef]

Disclaimer/Publisher's Note: The statements, opinions and data contained in all publications are solely those of the individual author(s) and contributor(s) and not of MDPI and/or the editor(s). MDPI and/or the editor(s) disclaim responsibility for any injury to people or property resulting from any ideas, methods, instructions or products referred to in the content.